American Mineralogist, Volume 87, pages 1727–1730, 2002

LETTER

Crystal morphology of MV-1 magnetite

SIMON J. CLEMETT,[1] KATHIE L. THOMAS-KEPRTA,[1,*] JOEL SHIMMIN,[2] MARY MORPHEW,[2] J. RICHARD MCINTOSH,[2] DENNIS A. BAZYLINSKI,[3] JOSEPH L. KIRSCHVINK,[4] SUSAN J. WENTWORTH,[1] DAVID S. MCKAY,[5] HOJATOLLAH VALI,[6] EVERETT K. GIBSON JR.,[5] AND CHRISTOPHER S. ROMANEK[7]

[1]Lockheed Martin Space Operations (NASA/Johnson Space Center Astrobiology Institute), 2400 NASA Road 1, Mail Code C23, Houston, Texas 77058, U.S.A.
[2]Department of Molecular, Cellular & Developmental Biology, University of Colorado, Boulder, Colorado 80309, U.S.A.
[3]Iowa State University, Department of Microbiology, 207 Science I, Ames, Iowa 50011, U.S.A.
[4]California Institute of Technology, Division of Geological and Planetary Sciences, 1200 East California Boulevard, Pasadena, California 91125, U.S.A.
[5]NASA, Johnson Space Center, Houston, Texas 77058, U.S.A.
[6]McGill University, Department of Earth and Planetary Sciences, 3450 University Street, Montreal, PQ H3A 2A7, Canada
[7]Savannah River Ecology Laboratory, Drawer E, University of Georgia, Aiken, South Carolina 29802, U.S.A.

ABSTRACT

Intracellular magnetite (Fe_3O_4) crystals produced by magnetotactic bacteria strain MV-1 are in the single-domain size range, and are chemically pure. We have previously suggested that they exhibit an unusual crystal habit described as truncated hexa-octahedral. Such a crystal morphology has not been demonstrated for any inorganic population of magnetite, nor would it be expected, given considerations of symmetry and free energy. By inference, this morphology is a physical signature of a biological origin. Here we report data from transmission electron microscope (TEM) tomography of such crystals isolated from magnetotactic bacteria, which confirm the unusual geometry, originally proposed from classical TEM tilt imaging.

INTRODUCTION

A subpopulation of magnetite crystals from the Martian meteorite ALH84001 has been interpreted as the product of relic biological activity based on their chemical and physical similarities to terrestrial magnetite produced by magnetotactic bacteria strain MV-1 (Thomas-Keprta et al. 2000, 2001). Of these similarities, one in particular has been the subject of considerable debate: the crystal morphology of MV-1 magnetite. Thomas-Keprta et al. (2001) have proposed that MV-1 magnetite displays an unusual crystal morphology, referred to as truncated hexa-octahedral, based on multi-tilt transmission electron microscope (TEM) imaging of individual magnetite crystals along multiple crystallographic axes. This geometry is not displayed by any known population of inorganic magnetite, nor would it be expected, based on the following two observations: (1) the point group symmetry of the magnetite unit cell is cubic of the point group type $\frac{4}{m}\bar{3}\frac{2}{m}$, whereas the point group symmetry for a truncated hexa-octahedron is trigonal of the type $\bar{3}\frac{2}{m}$; and, (2) the free energy minimized crystal geometry (i.e., Wulff polyhedron) of nanometer-sized magnetite is cubo-octahedral. Consequently, single-domain magnetite with a truncated hexa-octahedral geometry would seem to be the provenance of biogenic activity; as such, it would constitute a biosignature. Buseck et al. (2001) have argued that the approach of Thomas-Keprta et al. was insufficient to constrain crystal morphology and, additionally, that MV-1 magnetite does not display truncated hexa-octahedral geometry (P. Buseck, personal communication). They suggest, although they have not demonstrated, that only electron tomographic methods would be capable of determining the crystal morphology of MV-1 magnetite.

Here we report the crystal morphology exhibited by the majority of strain MV-1 magnetites as determined by TEM tomography. We are able to confirm the truncated hexa-octahedral model proposed by Thomas-Keprta et al. (2001).

CLASSICAL TEM ANALYSES OF MV-1 MAGNETITE

Magnetite is an Fe-suboxide (Fe_3O_4) that adopts the inverse spinel crystal structure and exhibits cubic symmetry. Magnetite nanocrystals have morphologies that represent a combination of cubic {100}, octahedral {111}, and dodecahedral {110} crystallographic faces. Based on simple surface free energy minimization arguments (Pimpinelli and Villain 1998), the equilibrium morphology of magnetite is expected to be a cubo-octahedron, and indeed, this is the most common form in which nanocrystalline magnetite is observed (Ichinose et al. 1992).

Thomas-Keprta et al. (2001) interpreted the morphology of MV-1 based on classical TEM imaging. This procedure involves imaging a single crystal with HRTEM over a wide angular range of tilt angles (±45°) with the caveat that this rotation must intersect two or more crystallographic zone axes. No *a priori* assumptions about the crystal morphology are necessary other than that of convexivity (invariably true for nanocrystals based on surface free energy minimization arguments). For each TEM image in the rotation sequence, the two-dimensional (2-D) projection of the crystal can be described by the intersection of a

* E-mail: kthomas@ems.jsc.nasa.gov

series of planes lying perpendicular to the image plane. The convex-hull (Barber et al. 1996) of the vertices defined by the intersection of three or more planes in three-dimensional (3-D) space describes the maximum volume polygon, whose projection under an identical rotation sequence is consistent with the experimental 2-D observations. For each zone axis observed, the 2-D plane that describes it can be colored according to its surface normal. If the surface normal lies coplanar with the {111} crystallographic directions, it is colored green, if coplanar with the {100} crystallographic directions, it is colored blue, and if coplanar with the {110} crystallographic directions, it is colored red. No distinction is made between a face, an edge, or a vertex, nor is one warranted, because an edge is simply a face of infinitesimal width, and a vertex is a face of infinitesimal length and width.

Clearly, if only a limited range of tilt angles, or a poorly chosen sequence of 2-D images is obtained, more than one polygon may account for the observation and the crystal morphology remains indeterminant. As such, care is necessary to use only those rotation sequences for which there is no ambiguity in the choice of model.

Using this approach, Thomas-Keprta et al. (2001) have posited that MV-1 magnetites have a geometry not previously described in the literature[1]. To avoid ambiguity, they had called this geometry "truncated hexa-octahedral" and represents the shape formed by eight octahedral {111} faces, six {100} faces, and six of a possible twelve {110} faces as indicated in Figure 1.

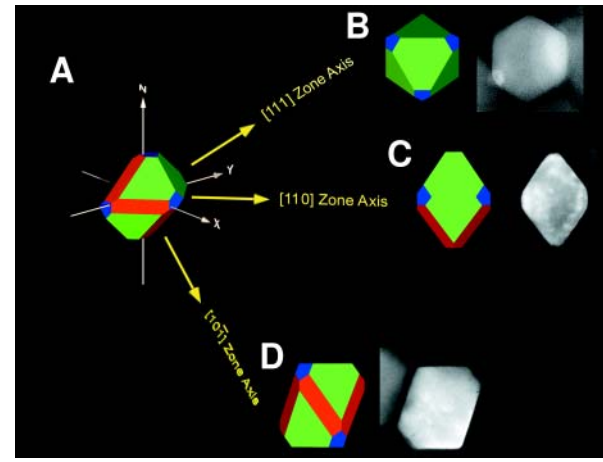

FIGURE 1. (A) An idealized truncated hexa-octahedral crystal of magnetite from the magnetotactic bacterium strain MV-1 displaying eight {111} octahedral (green) faces, six {1$\bar{1}$0} hexagonal (red) faces, and six {100} cubic (blue) faces. The majority of magnetite crystals isolated from magnetotactic bacteria strain MV-1 display this geometry. The principal cartesian axes x,y,z are indicated and in crystallographic nomenclature correspond to the [100], [010], [001] Miller indices. Directions for [111], [110], and [10$\bar{1}$] zone axes are shown by the yellow arrows. (B) View of an idealized truncated hexa-octahedron viewed down the [111] zone axis and the corresponding TEM image of a magnetite, ~50 nm in the longest dimension, from magnetotactic bacteria strain MV-1. Truncated hexa-octahedron viewed down the [111] axis of elongation displaying a hexagonal outline. (C) View of an idealized truncated hexa-octahedron viewed down the [110] zone axis and the corresponding TEM image of a magnetite, ~50 nm in the longest dimension, from magnetotactic bacteria strain MV-1. This view displays the width of both the {100} and {110} faces. (D) View of an idealized truncated hexa-octahedron viewed down the [10$\bar{1}$] zone axis and the corresponding TEM image of a magnetite, ~50 nm in the longest dimension, from magnetotactic bacteria strain MV-1.

TEM TOMOGRAPHIC ANALYSIS OF MV-1 MAGNETITES

The 3-D shape of an object can be reconstructed from a series of 2-D projections by any of several rigorous methods (Frank 1992). A principle that illustrates these methods is the Fourier Slice Theorem, which states that the Fourier transform of a 2-D projection from a 3-D object corresponds to a 2-D slice through the origin of the 3-D Fourier transform of that object. Thus, an approximation to the complete 3-D Fourier transform can be assembled from a large number of tilted views, and this approximation can be used to reconstruct the object in 3-D. Alternatively, real-space procedures, such as weighted back-projection, may be used to make reliable 3-D models from the multiple 2-D projections.

In the present study, we used a 300 KeV TEM with a field emission gun (Tecnai F-30 from FEI Inc.), equipped with a 2048 × 2048 pixel CCD camera from Gatan Inc. to image magnetite crystals[2] over tilt ranges from –50° to +58° in 2° tilt intervals. The images were aligned for back-projection by the positions of 5 nm Au spheres affixed to the specimen prior to microscopy (O'Toole et al. 1999). 3-D reconstructions were computed using weighted back-projection of the tilted views (Gilbert 1972). The tomograms were viewed and analyzed as a series of slices 0.525 nm thick, taken parallel to the specimen-supporting grid, using the IMOD software package (Kremer et al. 1996). The external shape of each magnetite crystal was determined by defining the external contour of a given magnetite in each slice and assembling a stack of these contours in 3-D.

To aid in visualization, the stacked contour array was reduced to an optimal mesh by Delaunay triangulation (Voronoi Diagrams and Delaunay Triangulations 1992). The surface normal to each of the triangles in the mesh was calculated and the triangle faces colored according to the orientation of that surface normal relative to the principal crystallographic axis of magnetite. Green surfaces correspond to {111} orientations, blue surfaces to {100} orientations, and red surfaces to {110} orientations as noted above. Triangles whose surface normal did not correspond to one of the principal axes were colored gray. This approach allows direct visual comparison of the reconstructed images to the geometric model previously proposed by Thomas-Keprta et al. (2001) (Figs. 2 and 3). Within the ex-

[1] In the microbiological community, strain MV-1 magnetites have been referred to previously as "parallelepipeds" (e.g., Mann et al. 1991), a term that does not adequately describe the true crystal morphology.

[2] Strain MV-1 cells were grown anaerobically with nitrous oxide as the terminal electron acceptor under heterotrophic conditions (Dean and Bazylinski 1999). MV-1 magnetite crystals were prepared for TEM analysis by extracting them from the cells and allowing an ~2 mL droplet of the magnetite suspension to dry on a continuous carbon TEM film supported by a copper grid.

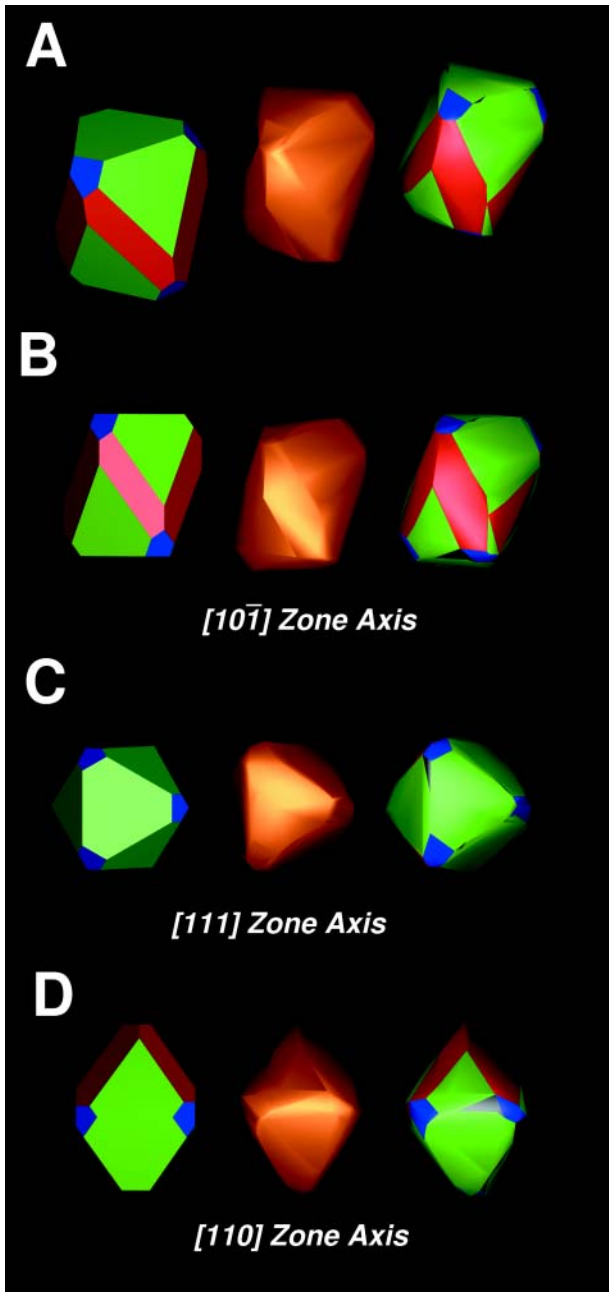

FIGURE 2. (A) From left to right, an idealized truncated hexa-octahedron, a reconstructed tomographic image of an MV-1 magnetite crystal created by Delaunay triangulation, and an indexed color reconstruction of the same tomographic image where the green surfaces correspond to a {111} orientation, blue surfaces to a {100} orientation and red surfaces to a {110} orientation. (The procedure used to determine the surface orientation, and hence color, of the tomographic model are described in the text.) Magnetite crystal shown in A-D is ~50 nm in length and has an aspect ratio of ~1.3. (B) Same as in A but viewed along the [10$\bar{1}$] zone axis (note similarity to Fig. 1D). (C) Same as in A but viewed along the [111] zone axis (note similarity to Fig. 1B). (D) Same as in A but viewed along the [110] zone axis (note similarity to Fig. 1C).

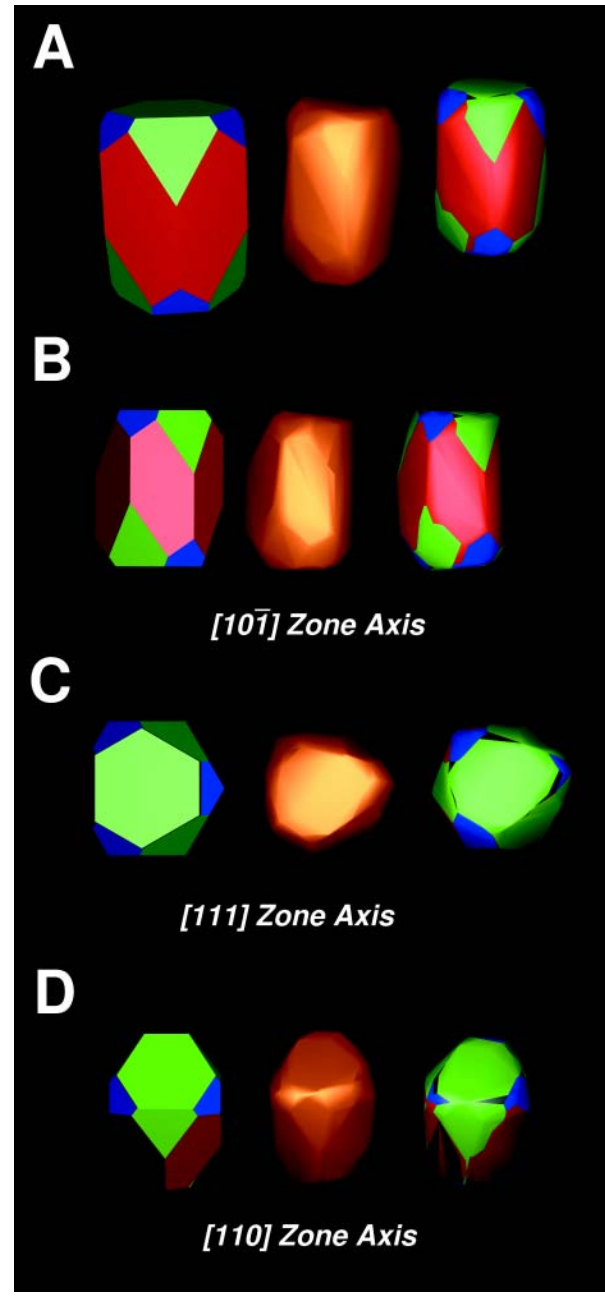

FIGURE 3. Same views as in Figure 2. Reconstruction of ~60 nm magnetite found in the same chain as the magnetite in Figure 2. While demonstrating truncated hexa-octahedral geometry, note the variation in the degree to which the individual faces are expressed compared to the magnetite in Figure 2. Such variations are commonly found among MV-1 magnetite crystals produced within the same cell (Thomas-Keprta et al. 2002).

perimental and numerical uncertainties of the deconvolution, the tomographic reconstruction is indistinguishable from the proposed truncated hexa-octahedral morphology of Thomas-Keprta et al. (2001) (Fig. 1).

CONCLUSIONS

The truncated hexa-octahedral geometry proposed by Thomas-Keprta et al. for MV-1 magnetites is consistent with the results obtained from TEM tomography. The classical TEM procedure used by Thomas-Keprta et al. is sufficient to constrain the 3-D morphology of a high symmetry crystallite such as magnetite, and may be a preferable method[3] to answer the highly specific question as to the morphology of biogenic MV-1 magnetite crystals. We note, however, that this approach is not suitable for a more generalized system that may involve low-symmetry, and/or non-convex morphologies; herein lies the advantage of tomographic techniques.

ACKNOWLEDGMENTS

We thank O. Clemett and N. Keprta for valuable suggestions. The manuscript was improved by the insightful comments of the reviews and the editor. This work was funded and supported by NASA's Astrobiology Institute and the Exobiology program.

REFERENCES CITED

Barber, C.B., Dobkin, D.P., and Huhdanpaa, H. (1996) The quickhull algorithm for convex hull. Applied and Computational Mathematics, Transactions on Mathmatical Software 22, 469–483.

Buseck, P.R., Dunin-Borkowski, R.E., Devouard, B., Frankel, R.B., McCartney, M.R., Midgley, P.A., Posfai, M., and Weyland, M. (2001) Magnetite morphology and life on Mars. Proceedings of the National Academy of Science, 98, 13490–13495.

Dean, A.J. and Bazylinski, D.A. (1999) Genome Analysis of Several Marine, Magnetotactic Bacterial Strains by Pulsed-Field Gel Electrophoresis. Current Microbiolog 39, 219–225.

Frank, J., Ed. (1992) Electron Tomography: Three-Dimensional Imaging with the Transmission Electron Microscope, 399 p. Plenum Press, New York.

Gilbert, P.F.C. (1972) The reconstruction of three-dimensional structure from projections and it application to electron microscopy. II. Direct methods. Proceedings of the Royal Society of London. B., Biological Sciences, 182, 89–102.

Ichinose, N., Ozaki, Y., and Kashu, S. (1992) Superfine Particle Technology (Chapter 1), p. 11–17. Springer Verlag, London.

Kremer, J.R., Mastronarde, D.N., and McIntosh, J.R. (1996) Computer visualization of three-dimensional image data using IMOD. Journal of Structural Biology, 116, 71–76.

Mann, S., Sparks, N.H.C., and Wade, V.J. (1991) Crystallochemical control of iron oxide biomineralization. In R.B. Frankel and R.P. Blakemore, Eds., Iron Biominerals, p. 21–47. Plenum Press, New York.

O'Toole, E.T., Winey, M., and McIntosh, J.R. (1999) High-voltage electron tomography of spindle pole bodies and early mitotic spindles in the yeast Saccharomyces cerevisiae. Molecular Biology of the Cell, 10, 2017–2031.

Pimpinelli, A. and Villain, J. (1998) The Equilibrum Crystal Shape In Physics of Crystal Growth, p. 43–59. Cambridge University Press, Cambridge.

Thomas-Keprta, K.L., Bazylinski, B.A., Kirchvink, J.L., Clemett, S.J., McKay, D.S., Wentworth, S.J., Vali, H., Gibson Jr., E.K., and Romanek, C.S. (2000) Elongated prismatic magnetite crystals in ALH84001 carbonate globules: Potential Martin magnetofossils. Geochimica et Cosmochimica Acta, 64, 4049–4081.

Thomas-Keprta, K.L., Clemett, S.J., Bazylinski, D.A., Kirschvink, J.L., McKay, D.S., Wentworth, S.J., Vali, H., Gibson, Jr., E.K., McKay, M.F., and Romanek, C.S. (2001) Truncated hexa-octahedral magnetite crystals in ALH84001: Presumptive biosignatures. Proceedings of the National Academy of Science, 98, 2164–2169.

Thomas-Keprta, K.L., Clemett, S.J., Bazylinski, D.A., Kirschvink, J.L., McKay, D.S., Wentworth, S.J., Vali, H., Gibson, E.K., and Romanek, C.S. (2002) Magnetofossils from Ancient Mars: A Robust Biosignature in the Martian Meteorite ALH84001. Applied and Environmental Microbiology, 68, 3663–3672.

Voronoi Diagrams and Delaunay Triangulations (1992). In D. Du and F. Hwang, Eds., Computing in Euclidean Geometry, Lecture Notes Series on Computing, vol. 1, 193–233. World Scientific, Singapore.

MANUSCRIPT RECEIVED MARCH 5, 2002
MANUSCRIPT ACCEPTED AUGUST 31, 2002
MANUSCRIPT HANDLED BY ROBERT F. DYMEK

[3] Large contrast variations are observed in bright field TEM images of high symmetry, periodic crystal structures due to interference effects associated with strong Bragg diffraction. This makes the tomographic reconstruction of single crystal magnetite particularly difficult. Any acquired rotation sequence must be oriented so as not to pass either near or through a principal zone-axis orientation.